An updated evaluation of the global mean Land Surface Air Temperature and Surface Temperature trends based on CLSAT and CMST

Qingxiang LI[1#], Wenbin Sun[1], Xiang YUN[2], Boyin HUANG[3], Wenjie DONG[1], Xiaolan L. WANG[4], Panmao ZHAI[2], Phil JONES[5]

1 School of Atmospheric Sciences and Guangdong Province Key Laboratory for Climate Change and Natural Disasters, SUN Yat-Sen University, Guangzhou, China

2 Chinese Academy of Meteorological Sciences, CMA, Beijing, China

3 National Centers of Environmental Information, NOAA, Asheville, USA

4 Climate Research Division, Environment and Climate Change Canada, Toronto, Canada

5 Climate Research Unit, University of East Anglia, Norwich, UK

 # Key Laboratory of Tropical Atmosphere-Ocean System (Sun Yat-sen University), Ministry of Education, and Southern Laboratory of Ocean Science and Engineering (Guangdong Zhuhai), Zhuhai, China

Submitted to ***Climate Dynamics***

Aug 2020

***Corresponding author:**

Dr. & Prof. Qingxiang Li
School of Atmospheric Sciences
Sun Yat-Sen University
Tangjiawan, Zhuhai Campus of SYSU
Zhuhai, China, 519082
Tel/Fax: 86-756-3668352
E-Mail: liqingx5@mail.sysu.edu.cn

Abstract

Past versions of global surface temperature (ST) datasets have been shown to have underestimated the recent warming trend over 1998-2012. This study uses a newly updated global land surface air temperature and land and marine surface temperature dataset, referred to as China global Land Surface Air Temperature (C-LSAT) and China Merged Surface Temperature (CMST), to estimate trends in the global mean ST (combining land surface air temperature and sea surface temperature anomalies) with the data uncertainties being taken into account. Comparing with existing datasets, the statistical significance of the global mean ST warming trend during the past century (1900–2017) remains unchanged, while the recent warming trend during the “hiatus” period (1998~2012) increases obviously, which is statistically significant at 95% level when fitting uncertainty is considered as in previous studies (including IPCC AR5) and is significant at 90% level when both fitting and data uncertainties are considered. Our analysis shows that the global mean ST warming trends in this short period become closer among the newly developed global observational data (CMST), with remotely sensed/Buoy network infilled datasets, and reanalysis data. Based on the new datasets, the warming trends of global mean land SAT as derived from C-LSAT 2.0 for the period of 1979-2019, 1951-2019, 1900-2019 and 1850-2019 were estimated to be 0.296, 0.219, 0.119 and 0.081 °C/decade, respectively. The warming trends of global mean ST as derived from CMST for the periods of 1998-2019, 1979-2019, 1951-2019 and 1900-2019 were estimated to be 0.195, 0.173, 0.145 and 0.091 °C/decade, respectively.

Keywords: Global Mean Surface Temperature (GMST); Global Land surface air temperature (GLSAT); Sea surface temperature (SST); Trends; Dataset

1. Introduction

The latest two IPCC scientific assessment reports (IPCC, 2007, 2013) pointed out that the warming of the climate system is unequivocal, The Global Mean Surface Temperature (GMST) is inferred from the land surface air temperature (LSAT) and sea surface temperature (SST) from in situ observations. Previous studies have shown that differences in the estimates of short-term trends are still relatively large, which prompted a debate within the climate community about a “hiatus” or “slowdown” in the warming over the 15 years following the 1997/1998 El Niño event (Cahill et al., 2015; Lewandowsky et al., 2015; Karl et al., 2015; Fyfe et al., 2016; Simmons et al., 2017; Rahmstorf et al., 2017; Medhaug et al., 2017; Lewandowsky et al., 2018; Risbey et al., 2018).

Over the past 30 years, several global LSAT datasets have been developed and have continuously been improved (Jones and Wigley, 2010; Hartmann et al., 2013; Hawkins and Jones, 2013). These include CRUTEM (Jones and Moberg, 2003; Jones et al., 2012), GHCN (Peterson and Vose, 1997; Smith and Reynolds, 2005; Smith et al., 2008; Lawrimore et al., 2011; Menne et al., 2019), GISTEMP (Hansen et al., 1999, 2001, 2006; Lessen et al., 2019), Berkeley Earth Surface Temperature (BEST) (Muller et al., 2013). Lugina et al (2006) and the Japan Meteorological Agency (JMA) also released their own datasets in recent years (http://ds.data.jma.go.jp/tcc/tcc/products/gwp/temp/ann_wld.html). With the continuous collection of climate data, improvements to data quality control and assurance technology and to the various spatio-temporal analysis methods, the trends of global/hemispheric mean LSATs have been updated by different research institutes (Hartmann et al., 2013). The demand for accurately estimating the magnitude of LSAT trends in monitoring climate change on global and regional scales is increasing day by day (Stott and Thorne, 2010). Recently, an international effort from China Sun Yat-Sen University (SYSU) and China Meteorological Administration (CMA), UK University of East Anglia (UEA), Environment and Climate Change Canada (ECCC), Australia Bureau of Meteorology (BOM) and USA State University of New York (SUNY) Albany published a new homogenized and integrated global LSAT dataset (C-LSAT), partly addresses this requirement (Xu et al., 2018).

Several SST data sets have also been developed by independent groups and are available for study, with several of these updated monthly or more frequently. Some analyses use only in situ observations, prominent examples being the Extended Reconstructed SST (ERSST; Smith et al., 1996; Huang et al., 2015, 2017a), UK Hadley SST version 3 and version 4 (HadSST3/4, Kennedy et al., 2011a; 2011b; 2019), and JMA's Centennial Observation-Based Estimates of SSTs (COBE-SST; Ishii et al., 2005), COBE-SST version 2 (COBE-SST2; Hirahara et al., 2014). The most recent ERSST version (ERSSTv5) and HadSST4 use newly released data archives from International Comprehensive Ocean-Atmosphere Data Set (ICOADS) 3.0 (Freeman et al., 2017), which improves SST spatial and temporal variabilities and absolute SST (Huang et al., 2017a, 2018). HadSST is used in HadCRUT and Berkley Earth (BE) analysis. ERSSTv5 is used in NOAAGlobalTempv5 (Zhang et al., 2019) and GISTEMP analyses.

IPCC's AR5 (IPCC, 2013) pointed out that, when updates have been made to all three GMST datasets (Hansen et al., 2010; Morice et al., 2012; Vose et al., 2012) used in AR4 (IPCC, 2007), GMSTs are in a somewhat better agreement with each other over recent years. For example, HadCRUT4 now has better sampling over the

Northern Hemisphere high latitude land areas (Jones et al.,2012; Morice et al., 2012), as comparisons with HadCRUT3 showed an underestimation of recent warming (Simmons et al., 2010). Recently, scientists have concluded that differences in the way that datasets handle data sparse areas such as the polar regions can result in a sampling "bias" of surface air temperature (SAT), especially in the so-called "hiatus" period during 1998-2012. (Cowtan and Way, 2014 and 2018; Karl et al., 2015; Huang et al., 2017a; Simmons et al., 2017). Cowtan and Way (2014) developed a hybrid version of global surface temperature: Satellite data were used to reconstruct an SAT series in the regions that are not covered by HadCRUT4 data (about 16% of global area by their evaluation, including parts of Africa and South America, so not just polar regions), which increases the temperature trend from 0.046°C/decade to 0.119°C/decade for the period of 1997-2012. Huang et al. (2017b) interpolated data from the International Arctic Buoy Observatory (IABO) data and found that the trend of warming was 0.112℃/decade over the period 1998-2012, which is higher than the trend in the NOAAGlobalTempv4 (formerly Merged Land and Ocean Surface Temperature dataset (MLOST)) data over the same period (about 0.050 °C/decade).

Also Zhang et al. (2019) showed that the updated surface temperature data tends to give a more consistent view of climate trends (from 0.070 °C/decade in v4 to 0.073 °C/decade in v5 during 1880-2018). Simmons et al. (2017) showed that the infilled observational datasets agreed better with both ERA-Interim and JRA-55 reanalysis and provided similar global mean surface warming trends since 1979, but their warming trends over 1998-2012 (0.140 and 0.090 °C/decade) were larger than any of the in situ observational datasets used in IPCC 5th Assessment Report (AR5) (Hartmann et al., 2013).

In this paper, we used a new merged global ST dataset- China Merged Surface Temperature, CMST (Yun et al., 2019; Li et al., 2020a) based on the most recently published C-LSAT (Xu et al., 2018) and ERSST v5 (Huang et al., 2017a) datasets, and conducted a systematic comparison of the global LSAT and ST trends during the "hiatus" or "slowdown" period (1998-2012) among the existing datasets. Based on these, we present a new evaluation of the global ST trends.

This paper is arranged as follows: the datasets and the methodology are briefly introduced in section 2; the update of the C-LSAT and the trends evaluation for different time scales are introduced in section 3; the analysis results are given in section 4; some reasons for the differences and uncertainty assessment of global ST changes are discussed in section 5, and the conclusions are presented in section 6.

2. Datasets and their processing methods

2.1 LSAT and SST datasets

A total of 14 data sources have been collected and integrated into the C-LSAT dataset including three global (CRUTEM4, GHCN, and Berkeley SAT), three regional sources and eight national sources (including homogenized datasets from Australia, Canada, China, and United States). Inhomogeneities in the data series are detected and adjusted for using a penalized maximal t-test (50% of all stations), then the station series are converted into 5 ° × 5 ° latitude by longitude grids data (for complete details see Xu et al., 2018). The C-LSAT version used in this paper includes the update described in Yun et al. (2019) and Li et al. (2020a), and will be detailed described in section 3. The newly updated China global Land Surface Air Temperature dataset (C-LSAT-2.0) is available at https://doi.pangaea.de/10.1594/PANGAEA.919574.

In this paper, several other LSAT datasets including Climatic Research Unit (CRU) CRUTEM4, NOAA Global Historical Climate Network dataset (GHCN) v3, Berkeley SAT and NASA GISTEMPv3 (all were downloaded in the first half of 2018 when the start of drafting this paper began, and most of the datasets have been updated during these two years) are also used to calculate/compare global LSAT trends. For consistency, the time periods for all the datasets have been set to Jan 1900 to Dec 2017 (since section 4). For CRUTEM4, we use the latest version CRUTEM4.6. GISTEMP has two versions with different degrees of spatial smoothing: 250km and 1200km. GISTEMP (1200km) starts in 1880 and GISTEMP (250km) starts in 1902. GHCNv3 has the same resolution as C-LSAT and CRUTEM4, and Berkeley SAT is at 1°×1° latitude by longitude resolution, which has been interpolated using Kriging methods.

Of the SST datasets mentioned in section 1, two (HadSST and ERSST) have been used to merge with LSAT to develop global ST datasets to assess global surface warming trends. ERSSTv5 (Huang et al., 2017a) uses new data sets from ICOADS Release 3.0 SST (Freeman et al., 2017), measurements from Argo floats down to 5 meters depth, and Hadley Centre Ice-SST version 2 (HadISST2) (Titchner and Rayner, 2013) ice concentrations. ERSSTv5 has improved SST spatial and temporal variability and absolute SST. HadSST3 is an ensemble dataset, the median of the 100 ensembles of HadSST3 is adopted to calculate the SST trends. For comparison, both of the two SST datasets have been used to merge with C-LSAT, respectively, in this paper.

2.2 Global ST datasets

After systematic comparisons, CMST was developed based on the C-LSAT and ERSSTv5 (Yun et al., 2019; Li et al., 2020a) and used to calculate long-term trends of GMST, similar to what was undertaken in Vose et al. (2012). The C-LSAT and ERSSTv5 are merged as follows: The monthly SSTs on 2°x2° grids and LSATs on 5°x5° grids are both first interpolated to 1°x1° grid, which is distributed in four grids of 1°x1° for SSTs and in 25 grids of 1°x1° for LSATs, and then box-averaged to 5°x5° deg grids according to the ratio between ocean and land areas for each individual grid box (Yun et al., 2019). The newly China global Merged Surface Temperature dataset (CMST) is available at https://doi.pangaea.de/10.1594/PANGAEA.919662.

The GMST series are calculated as follows: LSAT and SST anomalies are calculated relative to the reference period 1961-1990, and only those stations/grids with at least 15 years of values during 1961-1990 are calculated. The gridding of the land surface air temperature anomalies is undertaken by averaging all values within 5 ° × 5 ° grids (Jones and Moberg, 2003; Xu et al., 2018). Regional (North Hemisphere, South Hemisphere, and Tropics) series are calculated in the same way.

Four other global observation-based ST datasets including HadCRUT4, NOAAGlobalTempv4, Berkeley Earth (BE), and GISS v3 (downloaded in the first half of 2018) are also analyzed in this paper (each with time periods set to Jan 1900 to Dec 2017). Of these, BE provided two versions of merged global ST datasets, which differ in how the sea ice is treated. In the first version (BE1), temperature anomalies in the presence of sea ice are extrapolated from land-surface air temperature anomalies. In the second version (BE2), the anomalies are extrapolated from sea-surface water temperature anomalies (usually collected from open water areas near the periphery of the sea ice). It should be noted that all the global ST datasets have been updated since the publication of IPCC AR5, so the trends may be different from those published there, even if the version numbers have not been changed. For example, HadCRUT4 used an earlier version of CRUTEM4 in AR5, but CRUTEM4.6 at present; MLOST has been replaced by NOAAGlobalTempv4 since 2015, and also GISS has been updated several times on its use of SST datasets (currently, it uses ERSSTv5) and its uncertainty model (Lenssen et al., 2019).

Two other global ST analyses for shorter periods are also used in this paper. They are the comprehensively analyzed ECMWF ERA5 (Hersbach et al., 2020) and HadCRUT4 hybrid (Cowtan and Way, 2014). ERA5 provides a 2m temperature product from optimal-interpolation analyses of screen-level observations, using background fields provided by their main 4D-Var data assimilation schemes (with more observational data input along with CMIP5 greenhouse gases, volcanic eruptions, SST and sea-ice cover as the model input). In this study, we also used the ERA5 analysis fields over the land and the background fields over the oceans (https://climate.copernicus.eu/climate-bulletin-about-data-and-analysis) (Hersbach et al., 2020). The HadCRUT4 hybrid is the HadCRUT4 infilled using data from the University of Alabama in Huntsville (UAH) satellite data. Here, we use the median of the ensembles from HadCRUT4 as in Cowtan and Way (2014). Both of these two datasets cover the period from January 1979 to December 2017.

2.3 Estimation of trend and its uncertainty

The fitting uncertainty arises because there are many and various combinations of trend and noise that could have combined to give the observed series. Usually, the 95% confidence interval, expressed as $\beta \pm \delta$ for trend estimate β in this study, corresponds to the range of trends that have 5% or less chance of occurring by chance. This is based on the assumption that the annual temperature samples are approximately Gaussian distributed, but sample size also matters: The smaller the sample size, the more challenging it is to obtain good accuracy for trend estimates. Estimates of trend over a shorter period (like the period 1998-2012, in this paper) are thus more challenging. Similar to IPCC (2013), the long-term trend of global GMST and GMSAT and its significance under the 95% level (~1.96 sigma) are calculated by using the method of Restricted Maximum Likelihood Regression (REML, Diggle et al., 1994). The REML method is the basic method used to calculate climate change trend since IPCC TAR. Having the autocorrelation of temperature series been considered, it is more insensitive to extreme values than ordinary least squares. Therefore, it is more suitable to be used as a calculation method of climate change trend, especially for climate elements with autocorrelation such as temperature. So the trends and its uncertainties are mostly estimated based on REML (Tables 1-4).

However, recent studies (Cahill et al., 2015; Rahmstorf et al., 2017) state that almost every treatment of the significance of “hiatus” trends, including the IPCC reports, was based on an uncertainty method without consideration of part of the data uncertainties (the autocorrelation of the residual of linear fitting has not been considered) and has overestimated the significance of the change in trend. Although the existing global LSAT, SST datasets have generally been thought reliable, the uncertainties in global and regional ST during the past 100 years still attracts attention in recent studies (Brohan et al., 2006; Li et al., 2010; Kennedy et al., 2011a, b; Morice et al., 2012; Hartmann et al., 2013; Kennedy, 2014; Karl et al., 2015; Huang et al., 2015; 2017a; Li et al., 2017). According to Brohan et al. (2006) and Kennedy et al. (2011a; 2011b), uncertainties in the LSAT and SST are divided into 3 types: (1) station error (measurement error), (2) sampling error, and (3) bias error. Of these, the bias error is the most important at long-term and large scales and is the most clearly expressed in long-term trends in the global average for SST. Sampling errors are the most important at regional scales especially for the regions with relatively sparse observations (Li et al., 2020b; Li and Yang, 2019).

To compare with the significance of the GMST trends, in this study we estimated the data uncertainty using the spread of linear trends estimated from the time series that is perturbed by its standard deviation (STD) (Figure 1), following the similar approach of Karl et al. (2015) : (1) a time series is detrended; (2) the STD of the detrended time series is calculated; (3) a random temperature perturbation is selected based on a Gaussian distribution with zero mean and STD in (2); (4) a 1000-member ensemble time series is generated; (5) linear trend and its fitting uncertainty is calculated for all 1000 members; (6) the STD of the trend is defined as the data uncertainty, and the ensemble averaged fitting uncertainty is defined as the final fitting uncertainty; (7) the total uncertainty is defined as the root square mean of the data uncertainty and final fitting uncertainty. This provides an ensemble approach for evaluating the total uncertainties and the significance of the GMST trend. The results are given in Table 5.

3. Update of C-LSAT and its uncertainties evaluation

3.1 Interannual variation of LSAT anomaly and its uncertainty

Much progress has been made in the uncertainties estimation of the observational datasets (Brohan et al., 2006; Folland et al., 2001; Li et al., 2010; 2020a; Wang et al., 2014; Kent et al., 2017; Menne et al., 2018; Huang et al., 2019; Lesson et al., 2019) . The model produced by the Brohan et al. (2006) and Li et al. (2010) is used in this article. In this model uncertainties in the land data are divided into three types: (1) the uncertainties of individual station anomalies (station error); (2) the uncertainties in a grid box mean caused by estimating the mean from a small number of point values (sampling error); and (3) the uncertainties in large-scale temperatures caused by systematic changes in measurement methods (bias error). The total uncertainties value for any grid box can be obtained by adding the square root of the three errors.

Figure 2 shows the GLSAT anomaly and its 95% uncertainty range arising from station error, sampling error, bias error, and spatial coverage errors, and a comparison with the best estimate. It can be seen in the figure that the sampling error and station error have become smaller with time, and have remained stable after the 1950s. The greater uncertainty of the series in the first 50 years comes from insufficient data coverage; and the temperature series shows significantly larger inter-annual variability in the 50 years before the 20th century, due to the scarcity of station distribution. Inter-annual variability becomes much smaller after 1900, which is somewhat similar to China (Li et al., 2010; Li et al., 2017). The only difference is that the uncertainty of GLSAT is smaller than the regional scale average (Li et al., 2020b).

The GLSAT was mainly dominated by fluctuations from 1850s to the late 1970s. The series reached an extreme value (anomaly 0.18 ° C) in 1878, and then sharply decreased during the middle and late 1880s, after which, it rose to the late 1930s by fluctuations, and reached another extreme value (anomaly 0.26 ° C) in 1938 . The series then experienced a relatively cooling period to the mid-1960s, and then entered a continuously rapid warming period when it reached a new extreme value (anomaly 1.40 ° C) in 2016. It slightly declined in recent years, but remained high with the fourth (2017, anomaly 1.18 ° C), sixth place (2018, anomaly 0.96 ° C) and third place (2019, anomaly 1.24 ° C) since 1850s. If we calculate the difference between the

GLSAT anomalies in the last 10 years and those for the pre-industrial period (represented by the 1850-1900 averages), the number is 1.52 °C (about 1.40 °C for the last 20 years). That is, the GLSAT has now risen close to 1.5 °C from the pre-industrial period.

Judging from the 95% uncertainty range the GLSAT series (the inset of Figure 2a), the annual uncertainties were greater than 0.2 °C during the period of 1850 - 1880, after which they dropped to 0.15 °C and below during the period of 1881-1900; and after 1901 they dropped to 0.1 °C and below reaching their lowest value of about 0.07 °C after 1951. This result is very close to GISSTEMP, GHCN4, Bekeley SAT, and CRUTEM4 (Lesson et al., 2019), which also shows that the current accuracy is broadly similar among the existing GLSAT datasets in describing the GLSAT change (Li et al., 2020a).

3.2 Long-term trends of GLSAT and their uncertainties

The long-term trend of GLSAT anomaly from 1850 to 2019 and the 95% uncertainties range were calculated for several periods (Table 1). Regardless of whether only the fitting uncertainty is considered, or the fitting and data uncertainty are fully considered, the trends of LSAT changes in 1850-2019, 1901-2019, 1951-2019, 1979-2019 and 1998-2019 all significantly positive at 5% level, with the linear trends of 0.081 ± 0.014, 0.119 ± 0.023, 0.219 ± 0.042, 0.296 ± 0.077, and 0.234 ± 0.198 ° C per decade, respectively. Among these, since 1979, the surface air temperature has risen close to 0.3 ° C every 10 years, which is the period of fastest warming since the record began in the middle of the 19th century.

4. Comparison and evaluation on the global LSAT and ST trends

4.1 Comparisons on global LSAT and ST trends since 1998

4.1.1 Global LSAT changes

Xu et al. (2018) showed that C-LSAT obtained similar SAT trends to those in CRUTEM4 and GHCNv3 in continental areas for the period 1900-2014 (with faster warming rates in Asia and slower in Africa and Antarctica (1951-2014)) (Tables 5 and 6 in their paper). Figure 2 shows the distribution of the linear trends for SAT in all the grid boxes for the six datasets: C-LSAT, CRUTEM4.6, GHCNv3, GISTEMPv3 (200km and 1200km) and Berkeley SAT. GISTEMP and Berkeley SATs use similar station distributions to GHCNv3. It is worth mentioning that there are some strong spatial variations of some neighboring grid boxes for the shorter-term periods (Figure 3a), which is also occasionally found in other datasets (Figure 3 b-d), due to the different lengths of the data series in several grid boxes (Xu et al., 2018). Obviously, C-LSAT has the greatest coverage in comparison with other datasets especially in the higher latitude regions (Arctic and Antarctic) and the Tropics (30°S-30°N) (Figure 3; Xu et al., 2018 and Yun et al., 2019), except for GISTEMP (1200km smoothing) and Berkeley SAT due to spatial smoothing and infilling. C- LSAT includes more than 1,000 station data series in the Arctic (60°N-90°N), which is much more than used CRUTEM4 and GHCNv3/GISTEMPv3 (but no more data in the Antarctic) during 1998-2012 (Figures 2a-f). Figure 4 shows the annual mean LSAT anomaly series for C-LSAT, CRUTEM4, and GHCNv3 in the Arctic (land area in 60-90°N) and at global scales in all 5 datasets during 1998-2012 (1998-2017). In the Arctic, the linear trends of LSAT are calculated for different datasets as follows: 0.747, 0.798, and 0.559°C/decade, respectively (Figure 4a). The former two are much larger than the latter one, which agrees well with Cowtan and Way (2014) and Huang et al. (2017b). We also notice that the linear trend of LSAT has been changed to 0.080 °C/decade for

GHCNv4, which further shows the trend in this region was underestimated for GHCNv3 (0.052 °C/decade, Table 2).

At the global scale, the linear trends for LSAT are calculated for C-LSAT1.3, CRUTEM4.6, GHCNv3, GISTEMPv3, and BEST, respectively (Table 2). The global LSAT trends in GHCNv3 and Berkeley SAT are the smallest and the largest, respectively, which is related to the higher anomalies during 1998 to 2002 for GHCNv3 and for 2007 to 2012 for Berkeley SAT analysis. Only the trend in C-LSAT is significant at the 5% level. GISTEMPv3 shows lower anomalies during the whole 15-year period (Figure 4b).

Further, the trends of the 6 global mean LSATs for the different periods of 1998-2017, 1979-2017, 1951-2017, and 1900-2017 have been calculated and shown in Table 2. The trends for 1998-2017 are all significant at the 5% level. The LSAT trend from C-LSAT is higher than those derived from CRUTEM4.6, GHCNv3, and GISTEMPv3, but similar to that from Berkeley since 1998. The differences in the warming trends among all the datasets become smaller with the extension of the time scales.

4.1.2 Global ST changes

Of all the global ST datasets used in this paper, CMST, GISS and NOAAGlobalTemp use ERSST (CMST and GISSv3 use ERSSTv5, and NOAAGlobalTempv3 uses ERSSTv4, but the newly released NOAAGlobalTempv4 uses ERSSTv5 at present), HadCRUT4 and BE use 100 ensembles of HadSST3 (in this paper, we use the median of the 100 ensembles). Figure 5 shows the distribution of the linear trends of GMSTs in the period of 1998-2012 averaged over all available grid boxes in the six observational datasets and the other two datasets (HadCRUT Hybrid and ERA5). The main characteristics of the GMST trends are very similar to each other: Cooling trends are mostly found in East Asia (West Pacific Ocean), western North America including the northeastern North Pacific and the South Pacific. Warming trends are more significant in the high latitudes of the Northern Hemisphere. It should be noted that ST changes during the short-term period (1998-) have more differences than those during the longer periods (1900-, 1951- and 1979-). The latter show almost consistent warming trends at global scales (IPCC, 2007; 2013, also shown in Figure 9 of Xu et al. (2018).

Figure 6 shows the 6 observational global annual mean ST anomalies series, ERA5 ST series and HadCRUT Hybrid (with UAH) ST series over 1998-2012 (1998-2017) (all are relative to 1981-2010 averages). The linear trends of global ST are calculated for each dataset. They are 0.091, 0.055, 0.084, 0.071, 0.110, 0.079, 0.140, and 0.120°C/decade, respectively, in CMST, HadCRUT4, NOAAGlobalTempv3, GISSv3 (1200km), BE1, BE2, ERA5, and HadCRUT Hybrid (Table 3). Of these, HadCRUT4, GISSv3, BE2, and NOAAGlobalTempv3 (all the existing observational datasets) have similar warming trends, but lower than those during 1900-2017 and still insignificant at the 5% level. In contrast, ERA5, HadCRUT Hybrid and BE1 have much larger warming trends than others. BE1 has larger trends than BE2 because its temperature anomalies over the sea-ice area are extrapolated from land-surface air temperature anomalies (instead of the nearby sea-surface water temperature anomalies in BE2). Simmons et al. (2017) showed that the recent reanalysis (ERA-Interim: 0.140℃/decade, and JMA-55: 0.090℃/decade) exploited the richness of the observing system that has been in place over recent decades and extended the data coverage spatially. In this paper, our calculation indicates that the warming trends in the recently released ERA5 (Hersbach et al., 2020) were 0.140±0.112℃/decade (the same as with Simmons et al. (2017) using ERA-Interim) over the periods 1998-2012. This is slightly larger than that in CMST analysis (0.091±0.088℃/decade). Therefore, it is clear that the global "warming hiatus" trend is only a statistical artifact over this period of time, as Lewandowsky et al. (2015) and Cowtan et al. (2018) pointed out. Although Medhaug et al. (2017) and other studies pointed out that there was subduction of heat into the oceans during the period 1998-2012. From the current study, this heat subduction does not lead the “slowdown” of global warming rate.

Further, the CMST analyses show that the global ST warming rate for the period 1998-2017 is 0.190°C/decade, which is a little larger than that over 1979-2017, much larger than that over 1951-2017 (0.133°C/decade), and more than double the rate over 1900-2017 (0.086°C/decade) (Table 3). The most recent two years still continue to be warm years (2018 is the 5th warmest years, and 2019 is the 3rd warmest year), so the global ST warming rate for the period since 1998 (i.e. (1998 to 2019) would scarcely alter this evaluation (Li et al., 2020a).

4.2 Evaluation on Global and Hemispheric ST changes from CMST since 20th Century

4.2.1 Global Mean ST changes

According to IPCC AR5, GMST has increased since the late 19th century. Each of the past four decades has been significantly warmer than all the previous decades in the instrumental record, and the first and second decades of the 21st century have been the warmest two. For LSAT, Xu et al. (2018) discussed that the long-term trends for 1900-2014 evaluated from C-LSAT, CRUTEM4 and GHCNv3 are very close to each other. For Global ST change since 1880, IPCC AR5 listed 3 existing global observational datasets (HadCRUT4, NOAAGlobalTempv3 and GISSv3) and gave linear trends of 0.062 ± 0.012, 0.064 ± 0.015 and 0.065 ± 0.015°C/decade, respectively, for global mean ST changes over the period 1880-2012. Although the 1998-2017 warming trend is significantly higher in C-LSAT than all the other existing observational datasets except for Bekerley SAT, which uses a different gridding method, the global LSAT warming trends from C-LSAT over 1900-2017 are similar to CRUTEM4.6, GHCNv3 (also see the Figures 7, 8 in Xu et al. (2018)), GISTEMPv3, and Berkeley SAT analysis (Table 2). The global ST warming trends for 1900-2017 are also similar to each other for CMST, HadCRUT4, NOAAGlobalTemp, GISSv3, BE1 and BE2 (Table 3).

Further, we compared the GMST series derived from CMST with those derived from five other datasets during 1900-2017 and found that all the datasets agree well with each other on the surface temperature changes at the global scale in the past century, and the differences mainly exist at smaller spatial or temporal scales (Figure 7). Recently, we have confirmed that the consistency of the current GLSAT and GMST warming trends after 1880 is further strengthened (Li et al., 2020a).

Figure 8 shows the global, hemispheric and tropical-belty (30°S to 30°N) mean ST series based on CMST over the period of 1900-2019. Although with some spatial and temporal variability of local ST, CMST showed similar decadal and long-term changes to previous studies: the global mean ST experiences rapid warming during two periods: from 1910s to mid-1940s and from mid-1970s to present. The linear trends for global and regional ST change for different time periods are given in Table 4 and Table5. From Table 5, the estimated warming trends for global mean ST over

1900-2019 and 1951-2019 are 0.091°C/decade and 0.145°C/decade, respectively.

4.2.2 Hemispheric and Tropical Belt ST changes

Figures 8b-d show the Hemispheric and Tropical Belt ST changes during 1900-2019 based on CMST, with linear trends and their 95% uncertainties listed in Table 4. We noticed that for the NH and Tropics regions, the linear trends are continually increasing for the periods of 1900-2019, 1951-2019, 1979-2019, and 1998-2019, which shows the totally opposite results to what might be expected from the term "warming hiatus" over 1998-2012. Exceptions happen in the SH (the linear trends and their 95% confidence intervals are 0.077±0.006, 0.113±0.011, 0.079±0.022, and 0.125±0.055°C/decade for the period 1900-2019, 1951-2019, 1979-2019, and 1998-2019, respectively), which could be related to the recent cooling trends in the South Pacific region with lower warming rates over the Southern Hemisphere Oceans. It should be noted that the warming trend is greater (but with larger uncertainty) in the tropics than at global scales during the recent 20 years, which is different from that for longer term periods. The reason for the different warming trends between the tropics and global surface could be related to the relatively strong El Niño-Southern

Oscillation events in recent years (Trenberth et al., 2002; Zhai et al., 2015). Table 3 also shows that the differences between the warming rates in the NH and SH were getting larger during the last century. That is, the warming in NH and the Tropics is faster than that in the SH, which may change the balance of surface atmospheric energy (Peterson et al., 2011). This also shows that HadCRUT Hybrid possibly overestimating the warming trends since 1998 from the comparisons with CMST and other observational datasets (Figure 5 and their Figure 2 in Cowtan and Way (2014)), especially in the Southern Hemisphere.

5. Discussions

5.1 Differences due to data processing methods

All the datasets discussed above can be divided into two types: the first type is observational datasets without interpolation (or interpolated with small scanning radius), which includes C-LSAT (CMST), CRUTEM (HadCRUT4), GHCNv3 (NOAAGlobalTempv3), and GISTEMPv3-250km (GISS-250km). The other type includes all the interpolated/infilled datasets (Berkeley Earth (BE1, BE2), and GISTEMP-1200km (GISSv3-1200km)), infilled datasets (e.g., HadCRUT Hybrid), and reanalysis datasets (e.g., ERA5). It needs to be noted that GHCNv3 (NOAAGlobalTempv3) and GISTEMP-250km (GISSv3-250km) indeed contain a certain degree of interpolation, but the scanning radius of interpolation is small, which is insufficient to fill the grids of all missing data over large blank areas.

Cowtan and Way (2014) pointed out that the incomplete global coverage is a potential source of bias in global temperature reconstructions if the temperatures in the unsampled regions are not uniformly distributed over the planet's surface. The different interpolation/infilling (Kriging, UAH hybrid, IABO, Reanalysis, etc.) always leads to different results (see their Table 3). In this paper, although there are no direct relationships between the warming trends and interpolation methods, the trends are spatially relatively larger in GISSv3-1200km than those in GISSv3-250km (Figures 2d and 2e), but the trends are similar in GISTEMPv3-250km when compared with in GISTEMPv3-1200km.

A large difference is also seen between BE1 and BE2 (Table 3). This shows that the infilling of the temperature anomalies over the sea-ice region with land-surface air temperature anomalies increases the warming trends during recent decades

(1979-2017, 1998-2012 and 1998-2017). But it is interesting that the infilling decreases the trends during the longer periods (1900-2017; 1951-2017). This difference may be due to that some of the SAT data used in the infilling have been observed only during recent decades; these short ice SAT series increase the recent warming trends with better spatial sampling but were excluded when calculating long-term trends. This infilling possibly brings some inhomogeneities into the global/regional mean ST changes (and using UAH satellite data hybrid procedure would have a similar issue) as Xu et al. (2018) discussed. Therefore, the reconstruction of the long-term ST series in high latitudes is still open for discussion (Karl et al., 2015; Huang et al., 2017b).

Our study indicates that the difference of C-LSAT from CRUTEM, GHCNv3, and GISTEMPv3-250km results from the fact that the number of used stations in Asia, Arctic, Africa, and South America is much higher in C-LSAT than GHCNv3 but only slightly higher than CRUTEM4 for the entire analysis period. But the station densities in the latter 3 regions are still relatively low (figure 6 in Xu et al. (2018)). The differences among Global ST datasets are more complicated, but CMST obtains slightly larger trends than those from existing observational datasets, similar to those from ERA5, and closer to other reconstruction results with satellites.

5.2 The impact of SST analysis to the global mean ST trends

Measurements of SST have been made for more than 200 years for a wide variety of purposes. More complicated uncertainty quantification methods have been proposed for historic SST datasets than those with LSAT datasets (Kennedy, 2014, Kent et al., 2017; Huang et al., 2016, 2019). Previous studies pointed out that different SST analyses may be the main contributor of the inconsistencies of global STs (Simmons et al., 2017). Here we find similar features by analyzing the results of the global merged ST changes using ERSST5 and the median of the ensemble of HadSST3 (Figure 9). The result shows that the CMST (Merge1, C-LSAT+ERSSTv5) is colder than Merge2 (C-LSAT + median of HadSST3) during 1920s -1970s, and from 2000s to present, but the long-term trends for different merging methods (for the period of 1900-2017) remain similar. These results are very similar to the differences between the HadSST3 and ERSSTv4 described in Figure 9a of Huang et al. (2016). There are some differences, however, in the trends over the longer time periods since

1900, which is related to the SSTs being higher in HadSST3 than ERSSTv5 due to higher ship SST bias corrections in the 1880s–1940s and 1950s–1960s as indicated in Huang et al. (2016).

The linear trends and their 95% uncertainty ranges for global ST series based on the two different merged datasets are listed in Table 5. It is interesting that the warming trends in CMST are all larger than those in Merge2 in different periods except for the period of 1979-2017. This is obvious because the ST anomalies in each start year (1900, 1951 and 1998) are lower than those in the Merge2 series. That is, if we choose other start years (for example, 1979, 1981 etc.), the results could alter the opposite way. Although there are some differences in the global mean ST trends during the period of 1998-2012 between the two merges, the significances of the trends are quite similar. In addition, we noticed that the differences between the merging methods are not more than the 95% of the linear trends fitting uncertainty range.

5.3 Significance when considering both the data and fitting uncertainties

Note that the trend uncertainties given in the Tables 1-4 are only the fitting uncertainties. An ensemble approach has been adopted to better describe complex temporal and spatial interdependencies of measurement and bias uncertainties and to allow these correlated uncertainties to be taken into account when the time series is perturbed by data uncertainty in HadCRUT4 (Morice et al., 2012). Correlated errors in the station series are quantified by running the homogenization algorithm as an ensemble in GHCNv4 (Menne et al., 2018). The uncertainties from both C-LSAT and ERSSTv5 are evaluated, respectively, and then these two are combined into the total uncertainties of CMST (Li et al., 2020a).

After the data uncertainties are propagated into the uncertainty of trend calculation, the significance of the GMST trends for different scales mostly remains the same, except for the trend for the period of 1998-2012, which has changed from 0.091±0.088°C/decade (significant) when only trend fitting uncertainty is included to 0.091±0.094°C/decade (insignificant at the 95% level but significant at the 90% level) when the fitting and data uncertainties are also included (Table 5). This shows that the traditional evaluation on the uncertainties indeed overestimated the significance of trends of 1998-2012, in agreement with the previous studies (Cahill et al., 2015;

Rahmstorf et al., 2017). This trend is slightly larger than those derived from existing observational datasets in HadCRUT4, NOAAGlobalTemp, GISSv3 (1200), and BE2 (Berkeley dataset with SST in Polar Region) respectively. It is closer to that from ERA5, Karl et al. (2015), and the other reconstruction data sets with satellite and other kinds of observations (Cowtan and Way, 2014; Huang et al., 2017a).

6. Conclusion

The recently released C-LSAT dataset, with more stations at higher latitudes and improved data quality at sub-continental scales, shows broad consistency with the recent analyses of recent global LSAT changes. The trends of global mean land SAT as derived from C-LSAT2.0 for the period of 1979-2019, 1951-2019, 1900-2019 and 1850-2019 were estimated to be 0.296, 0.219, 0.119 and 0.081 °C/decade, respectively.

When this data was merged with ERSSTv5, we have produced the new merged global ST dataset, CMST (Yun et al., 2019; Li et al., 2020a). The updated results show that the significance of the global ST warming trend over the past century (1900–2017) remains the same as previous estimates, and that the recent warming trend since 1998 increases slightly and is statistically significant. Using the new dataset CMST, the trend of global mean STs over the period 1998-2012 was estimated to be a little higher than that of other existing datasets and more significant: It is 0.091 ± 0.094°C/decade when both the fitting and data uncertainties were considered, and 0.091 ± 0.088°C/decade when only the fitting uncertainty was considered as in the AR5 IPCC report. This suggests that the recent temperature changes (including those record warm years at the end of the series) have likely brought the debate about the "warming hiatus" to an end. This is opposite to the previous understanding as described in IPCC AR5 and many other studies (but the AR5 does include a brief discussion on the uncertainty of trend in B.1 of the Summary for Policy Makers) (IPCC, 2013b).

Using these new datasets, we have presented an updated evaluation of global and hemispheric ST changes since 1900. When both the fitting and data uncertainties were considered, the warming trends of global mean STs for the periods 1900-2019, 1951-2019, 1979-2019, and 1998-2019 are estimated to be 0.091 ± 0.011, 0.145 ± 0.019, 0.173 ± 0.033, and 0.194 ± 0.083 °C/decade, respectively (0.091±0.008, 0.145±0.014, 0.173±0.026 and 0.195 ± 0.063 °C/decade when only the fitting uncertainty was considered).

The introduction of newly adjusted sea surface temperature (SST) data (Karl et al., 2015), with record-setting extreme global temperature for the recent six years (2014-2019), makes the formulation of the "warming hiatus" gradually fade away. The newly released C-LSAT and CMST datasets support these results by increasing the warming trends during the period 1998-2012 (and of 1998-2017) than those in the previous versions of other existing observational datasets. However, more consistent trends have been found from the datasets when applying sampling bias correction using satellites, SAT observation in buoys, and reanalysis, which need to be more comprehensively validated in future with more new observations and improved reanalysis.

Acknowledgment

This study is supported by the Natural Science Foundation of China (Grant: 41975105), the National Key R&D Program of China (Grant: 2018YFC1507705; 2017YFC1502301). And thanks

Dr. Geert van Oldenborgh from Royal Netherlands Meteorological Institute (KNMI) for providing several global SAT/ST datasets on Climate Explorer website (http://climexp.knmi.nl/) for calculating the temperature change trends in this paper.

Reference

Brohan P, Kennedy JJ, Harris I, Tett SFB, Jones PD. (2006) Uncertainty estimates in regional and global observed temperature changes: A new dataset from 1850. J. Geophys. Res. 111: D12106, doi: 10.1029/2005JD006548.

Cahill N, S Rahmstorf and A Parnell, (2015) Change points of global temperature Environ. Res. Lett. 10 084002, doi:10.1088/1748-9326/10/8/084002

Cowtan, K. & Way R. G. (2014) Coverage bias in the HadCRUT4 temperature series and its impact on recent temperature trends, Quarterly Journal of Royal Meteorological Society, 140, 1935–1944. doi:10.1002/qj.2297

Cowtan K, P Jacobs, P Thorne et al, (2018) Statistical analysis of coverage error in simple global temperature estimators, Dynamics and Statistics of the Climate System, 1–18 doi:10.1093/climsys/dzy003

Dee D. P., Uppala S. M., Simmons A. J., Berrisford P., Poli P., Kobayashi S., Andrae U., Balmaseda M. A., Balsamo G., Bauer P., Bechtold P., Beljaars A. C. M., van de Berg L., Bidlot J., Bormann N., Delsol C., Dragani R., Fuentes M., Geer A. J., Haimberger L., Healy S. B., Hersbach H., H´olm E. V., Isaksen L., K°allberg P., K¨ohler M., Matricardi M., McNally A. P., Monge-Sanz B. M., Morcrette J. J., Park B. K., Peubey C., de Rosnay P., Tavolato C., Th´epaut J. N., Vitart F. (2011) The ERA-Interim reanalysis: Configuration and performance of the data assimilation system. Q. J. R. Meteorol. Soc. 137: 553–597, doi: 10.1002/qj.828.

Diggle P J, Liang K Y, Zeger S L. (1994) Analysis of Longitudinal Data. Oxford University Press.

Freeman, E., and Coauthors, (2017) ICOADS Release 3.0: A major update to the historical marine climate record. International J. Climatology, 37, 2211–2232, DOI: 10.1002/joc.4775.

Folland, C. K., and Coauthors , 2001: Observed climate variability and change. Climate Change 2001: The Scientific Basis, J. T. Houghton et al., Eds., Cambridge University Press, 99–181.

Fyfe JC, Meehl GA, England MH, Mann ME, Santer BD, Flato GM, Hawkins E, Gillett NP, Xie S-P, Kosaka Y, Swart NC. (2016) Making sense of the early-2000s warming slowdown. Nat. Clim. Change 6: 224–228, doi: 10.1038/nclimate2938.

Hansen J, Ruedy R, Glascoe J et al. (1999), GISS analysis of surface temperature change. J. Geophys.

Res., 104: 30997-31022.

Hansen J, Ruedy R, Sato M et al. (2001), A closer look at United States and global surface temperature change. J. Geophys. Res., 106: 23947-23963.

Hansen, J., M. Sato, R. Ruedy, K. Lo, D. W. Lea, and M. Medina Elizade (2006), Global temperature change, Proc. Natl. Acad. Sci. U. S. A., 103, 14, 288–293, doi:10.1073/pnas.0606291103

Hansen J， R Ruedy ， M Sato ， K Lo (2010), Global surface temperature change，Reviews Of Geophysics , 48 (4) ，RG404:1-29，DOI: 10.1029/2010RG000345

Hartmann, D. L. In: Climate Change (2013) The Physical Science Basis. (eds Stocker, T. F. et al.), Ch. 2 (Cambridge University Press, Cambridge, 2013).

Hawkins E D and Jones P D, (2013) Notes and Correspondence On increasing global temperatures: 75 years after Callendar, Q. J. R. Meteorol. Soc. 139: 1961–1963

Hersbach, H., Bell, B., Berrisford, P., Hirahara, S., Horányi, A., Muñoz-Sabater, J., et al. (2020). The ERA5 Global Reanalysis. Quarterly Journal of the Royal Meteorological Society. doi:10.1002/qj.3803

Hirahara, S., M. Ishii, and Y. Fukuda, (2014) Centennial-scale sea surface temperature analysis and its uncertainty. J. Climate, 27, 57–75, doi:10.1175/JCLI-D-12-00837.1.

Huang B, MJ Menne, T Boyer, E Freeman, et al, (2019) Uncertainty estimates for sea surface temperature and land surface air temperature in NOAAGlobalTemp version 5, J. Climate, doi : 10.1175/CLI-D-19-0395.1, in press.

Huang, B., P. W. Thorne, T. M. Smith, W. Liu, J. Lawrimore, V. F. Banzon, H.-M. Zhang, T. C. Peterson, and M. Menne, (2016) Further exploring and quantifying uncertainties for Extended Reconstructed Sea Surface Temperature (ERSST) version 4 (v4). J. Climate, 29, 3119-3142, DOI: 10.1175/JCLI-D-15-0430.1.

Huang, B., W. Angel, T. Boyer, L. Cheng, G. Chepurin, E. Freeman, C. Liu, and H.-M. Zhang, (2018) Evaluating SST analyses with independent ocean profile observations. J. Climate, 31, 5015-5030, doi:10.1175/jcli-d-17-0824.1.

Huang, B., P. Thorne, V. Banzon, T. Boyer, G. Chepurin, J. Lawrimore, M. Menne, T. Smith, R. Vose, and H. Zhang, (2017a) Extended Reconstructed Sea Surface Temperature version 5 (ERSSTv5): Upgrades, Validations, and Intercomparisons. J. Climate. 30, 8179-8205, doi:10.1175/JCLI-D-16-0836.1.

Huang，J., Zhang，X., Zhang，Q., et al. (2017b) Recently Amplified Arctic Warming Has Contributed to a Continual Global Warming Trend ， Nature Climate Change, 7, 875–879.

doi:10.1038/s41558-017-0009-5.

IPCC. 2007. Climate Change (2007) The Physical Science Basis. Contribution of Working Group I to the Fourth Assessment Report of the Intergovernmental Panel on Climate Change, Solomon S, Qin D, Manning M, Chen Z, Marquis M, Averyt KB, Tignor M, Miller HL. (eds.): 996 pp. Cambridge University Press: Cambridge, UK and New York, NY.

IPCC. 2013a. Climate Change (2013) The Physical Science Basis. Contribution of Working Group I to the Fifth Assessment Report of the Intergovernmental Panel on Climate Change, Stocker TF, Qin D, Plattner G-K, Tignor M, Allen SK, Boschung J, Nauels A, Xia Y, Bex V, Midgley PM. (eds.): 1535 pp. Cambridge University Press: Cambridge, UK and New York, NY.

IPCC, 2013b. Summary for Policymakers. In: Climate Change (2013) The Physical Science Basis. Contribution of Working Group I to the Fifth Assessment Report of the Intergovernmental Panel on Climate Change [Stocker, T.F., D. Qin, G.-K. Plattner, M. Tignor, S.K. Allen, J. Boschung, A. Nauels, Y. Xia, V. Bex and P.M. Midgley (eds.)]. Cambridge University Press, Cambridge, United Kingdom and New York, NY, USA

Ishii, M., A. Shouji, S. Sugimoto, and T. Matsumoto, (2005) Objective analyses of sea-surface temperature and marine meteorological variables for the 20th century using ICOADS and the Kobe

Collection. Int. J. Climatol., 25, 865–879, doi:10.1002/ joc.1169.

Jones P. D., L. David, T. J. Osborn, C. Harpham, M. Salmon, and C. P. Morice (2012), Hemispheric and large-scale land-surface air temperature variations: An extensive revision and an update to 2010. J Geophys Res-Atmos, 117, doi:10.1029/2011JD017139.

Jones, P. D., and T. M. L. Wigley (2010), Estimation of global temperature trends: What's important and what isn't, Clim. Change, 100(1), 59–69.

Jones P. D., Moberg A. (2003) Hemispheric and large-scale surface air temperature variations: an extensive revision and an update to 2001, J Climate, 16:206–223

Karl T.R., Arguez A., Huang B., Lawrimore J.H., McMahon J.R., Menne M.J., Peterson T.C., Vose R.S., Zhang H.M. (2015) Possible artifacts of data biases in the recent global surface warming hiatus. Science,348: 1469–1472. doi:10.1126/science.aaa5632

Kennedy, J. J., N. A. Rayner, R. O. Smith, D. E. Parker, and M. Saunby, (2011a) Reassessing biases and other uncertainties in sea surface temperature observations measured in situ since 1850: 2. Biases and homogenization. Journal of Geophysical Research-Atmospheres, 116, D14104, doi:10.1029/2010JD015220

Kennedy, J. J., N. A. Rayner, R. O. Smith, M. Saunby, and D. E. Parker (2011b) Reassessing biases and other uncertainties in sea surface temperature observations since 1850, part 1: Measurement and sampling uncertainties. J. Geophys. Res., 116. D14103, doi:10.1029/2010JD015218

Kennedy, J. J. (2014) A review of uncertainty in in situ measurements and data sets of sea surface temperature, Rev. Geophys., 52, 1–32, doi:10.1002/2013RG000434.

Kennedy, J. J., Rayner, N. A., Atkinson, C. P., & Killick, R. E. (2019) An ensemble data set of sea-surface temperature change from 1850: the Met Office Hadley Centre HadSST.4.0.0.0 data set. Journal of Geophysical Research: Atmospheres, 124. https://doi.org/10.1029/2018JD029867

Kent, E. C., Kennedy, J. J., Smith, T. M., Hirahara, S., Huang, B., Kaplan, A., Parker, D. E., Atkinson, C. P., Berry, D. I., Carella, G., Fukuda, Y., Ishii, M., Jones, P. D., Lindgren, F., Merchant, C. J., Morak-Bozzo, S., Rayner, N. A., Venema, V., Yasui, S., Zhang, H-M. (2017) A call for new approaches to quantifying biases in observations of sea-surface temperature. *Bulletin of the American Meteorological Society*, **98**, 1601-1616, doi:10.1175/BAMS-D-15-00251.1

Lawrimore J. H., M. J. Menne, B. E. Gleason, C. N. Williams, D. B. Wuertz, R. S. Vose, and J. Rennie (2011) An overview of the Global Historical Climatology Network monthly mean temperature data set, version 3. Journal of Geophysical Research-Atmospheres, 116, doi:10.1029/2011jd016187.

Lenssen, N., G. Schmidt, J. Hansen, M. Menne,A. Persin,R. Ruedy, and D. Zyss, (2019) Improvements in the GISTEMP uncertainty model. Journal of Geophysical Research-Atmospheres, 124, 12, 6307-6326, doi:10.1029/2018JD029522.

Lewandowsky S., K Cowtan., J. Risbey, et al. (2018) The ‘pause’ in global warming in historical context: (II). Comparing models to observations. Envion. Res. Lett., 13, 123007, https://doi.org/10.1088/1748-9326/aaf372.

Lewandowsky S., J. Risbey, and N. Oreskes (2016) The “pause” in global warming: Turning a routine fluctuation into a problem for science. Bull. Amer. Meteor. Soc., 97, 723–733, doi:10.1175/BAMS-D-14-00106.1.

Li Q. and Y. Yang, (2019) Comments on “Comparing the current and early 20th century warm periods in China” by Soon W., R. Connolly, M. Connolly et al., Earth‐Science Reviews, 198， 102886, https://doi.org/10.1016/j.earscirev.2019.102886

Li Q., Zhang L.，Xu W. et al. (2017) Comparisons of time series of annual mean surface air temperature for China since the 1900s：Observation, Model simulation and extended reanalysis. Bull. Amer. Meteor. Soc.，98 (4):699-711, doi: 10.1175/BAMS-D-16-0092.1

Li Q., S. Yang, W. Xu, X. L. Wang, P. Jones, D. Parker, L. Zhou, Y. Feng, and Y. Gao (2015) China experiencing the recent warming hiatus, Geophys. Res. Lett., 42, doi:10.1002/2014GL062773.

Li Q., W. Dong, W. Li, X. Gao, P. Jones, J. Kennedy and D. Parker (2010) Assessment of the uncertainties in temperature change in China during the last century. Chin. Sci. Bull., 55, 1974-1982, doi: 10.1007/s11434-010-3209-1.

Li Q, Sun W, Huang B, Dong W, Wang X, Zhai P and P. Jones. (2020a) Consistency of global warming trends strengthened since 1880s, Science Bulletin, accepted.

Li Q., W. Dong and P. Jones (2020b) Continental Scale Surface Air Temperature Variations: An Experience Derived from China Region Practice, Earth-Science Reviews, 200, 998, https://doi.org/10.1016/j.earscirev.2019.102998.

Lugina, K. M., P. Y. Groisman, K. Y. Vinnikov, V. V. Koknaeva, and N. A. Sperandkaya (2006), Monthly surface air temperature time series area-averaged over the 30-degree latitudinal belts of the globe, 1881–2005, in Trends: A Compendium of Data on Global Change [online], doi:10.3334/CDIAC/cli.003, Carbon Dioxide Inf. Anal. Cent., Oak Ridge Natl. Lab., U.S. Dep. Of Energy, Oak Ridge, Tenn. (Available at http://cdiac.ornl.gov/trends/temp/lugina/lugina.html)

Medhaug I, Stolpe M, Fischer E et al. (2017) Reconciling controversies about the 'global warming hiatus, Nature, 545: 41-47. DOI:10.1038/nature22315.

Morice, C. P., J. J. Kennedy, N. A. Rayner, and P. D. Jones (2012) Quantifying uncertainties in global and regional temperature change using an ensemble of observational estimates: The HadCRUT4 dataset, J. Geophys. Res., 117, D08101, doi:10.1029/2011JD017187.

Menne J. M., C. N. Williams, B. E. Gleason, et al. (2018) The Global Historical Climatology Network Monthly Temperature Dataset, Version 4, J Climate, 31 (24): 9835–9854. https://doi.org/10.1175/JCLI-D-18-0094.1

Muller, R. A., J. Curry, D. Groom, R. Jacobsen, S. Perlmutter, R. Rohde, A. Rosenfeld, C. Wickham, and J. Wurtele (2013) Decadal variations in the global atmospheric land temperatures, J. Geophys. Res. Atmos., 118, doi:10.1002/jgrd.50458.

Peterson T.C., and R.S. Vose (1997) An overview of the Global Historical Climatology Network temperature database. Bulletin of the American Meteorological Society, 78, 2837-2849.

Peterson T. C., Willett K. M., Thorne P. C. (2011) Observed changes in surface atmospheric energy over land. Geophys. Res. Lett. 38: L16707, doi:10.1029/2011GL048442.

Rahmstorf S, G Foster and N Cahill (2017) Global temperature evolution: recent trends and some pitfalls. Environ. Res. Lett., 12 054001, https://doi.org/10.1088/1748-9326/aa6825

Rayner, N. A., P. Brohan, D. E. Parker, C. K. Folland, J. J. Kennedy, M. Vanicek, T. J. Ansell, and S. F. B.

Tett (2006) Improved analyses of changes and uncertainties in sea-surface temperature measured in-situ since the mid-nineteenth century, J. Clim., 19, 446 – 469.

Risbey J., S. Lewandowsky, K Cowtan., et al. (2018), A fluctuation in surface temperature in historical context: reassessment and retrospective on the evidence. Envion. Res. Lett., 13, 123008, https://doi.org/10.1088/1748-9326/aaf342.

Rohde R., Muller, R. A., Jacobsen, R., et al. (2013), A new estimate of the average earth surface land temperature spanning 1753 to 2011. Geoinfor Geostat: An Overview. doi:10.4172/gigs.1000101.

Simmons, A.J., Berrisford, P., Dee, D.P., Hersbach, H., Hirahara, S. and Thépaut, J.N. (2017) A reassessment of temperature variations and trends from global reanalyses and monthly surface climatological datasets. Quarterly Journal of the Royal Meteorological Society, 143*: 101-119,*. doi: https://doi.org/10.1002/qj.2949

Simmons AJ, Willett KM, Jones PD, Thorne PW, Dee DP. (2010). Low-frequency variations in surface atmospheric humidity, temperature and precipitation: Inferences from reanalyses and monthly gridded observational datasets. J. Geophys. Res. 115: D01110, doi: 10.1029/2009JD012442.

Stott, P.A. & Thorne, P.W. (2010) How best to log local temperatures? Nature, 465:158-159.

Smith, T., R. W. Reynolds, R. E. Livezey, and D. C. Stokes (1996) Reconstruction of historical sea surface temperatures using empirical orthogonal functions. J. Climate, 9, 1403–1420, doi:10.1175/1520-0442(1996)009,1403: ROHSST.2.0.CO;2.

Smith, T. M., and R. W. Reynolds (2005) A global merged land-air-sea surface temperature reconstruction based on historical observations (1880–1997), J. Clim., 18, 2021–2036, doi:10.1175/JCLI3362.1.

Smith, T., R. W. Reynolds, T. C. Peterson, and J. Lawrimore (2008) Improvements to NOAA’s historical merged land–ocean surface temperature analysis (1880–2006). J. Climate, 21, 2283–2296, doi:10.1175/2007JCLI2100.1

Titchner, H. A., and N. A. Rayner (2014) The Met Office Hadley Centre sea ice and sea surface temperature data set, version 2: 1. Sea ice concentrations, J. Geophys. Res. Atmos., 119, 2864-2889, doi: 10.1002/2013JD020316.

Trenberth K. T., P. Stepaniak, and S. Worley (2002) Evolution of El Niño -Southern Oscillation and global atmospheric surface temperatures, J. Geophys. Res. 107, D8, 4065, 10.1029/2000JD000298

Vose, R. S., et al. (2012) NOAA's Merged Land-Ocean Surface Temperature Analysis. Bulletin of the American Meteorological Society, doi:10.1175/BAMS-D-11-00241.1.

Xu W., Q. Li, P. D. Jones, X. L. Wang, et al. (2018) A new integrated and homogenized global monthly land surface air temperature dataset for the period since 1900, Clim. Dynamics, 50:2513-2536, 10.1007/s00382-017-3755-1.

Yun, X., Huang, B., Cheng, J., Xu, W., Qiao, S., and Li, Q. (2019) A new merge of global surface temperature datasets since the start of the 20th Century, Earth Syst. Sci. Data, 11, 1629–1643, https://doi.org/10.5194/essd-11-1629-2019

Zhai P., Yu. R., Guo Y., Li Q., Ren X., Wang Y., Xu W., Liu Y., Ding Y. (2016) The strong El Niño in 2015/2016 and its dominant impacts on global and China’s climate. J. Meteorol. Res., 74(3): 309–321. doi:10.11676/qxxb2016.049

Zhang, H.-M., J. H. Lawrimore, B. Huang, M. J. Menne, X. Yin, A. SÃ¡nchez-Lugo, B. E. Gleason, R. Vose, D. Arndt, J. J. Rennie, and C. N. Williams, (2019) Updated temperature data give a sharper view of climate trends. EOS, 100, doi:10.1029/2019EO128229.

List of Tables

Table 1. Long-term trends and uncertainty of global land temperature over the indicated periods (°C / 10a)

Table 2. Century-scale trends in global LSAT change from different datasets（°C / decade）

Table 3. Century-scale trends in annual global ST change from different datasets（°C / decade）

Table 4. Century-scale trends in global, Hemispheric and Tropical Belt ST change（°C / decade）

Table 5. GMST change trends (different uncertainties evaluation) with different SST datasets（°C / decade）

Table1 Long-term trends and uncertainty of global land temperature over the indicated periods (° C / 10a)

Period	**Warming periods**			
	1850-2019	1901-2019	1951-2019	1979-2019
Trend	0.081±0.014	0.119±0.023	0.219±0.042	0.296±0.077

Table 2. Century-scale trends in global LSAT change from different datasets（°C / decade）

	1900-2017	1951-2017	1979-2017	1998-2017	1998-2012
C-LSAT	0.100±0.012	0.188±0.024	0.274±0.040	0.247±0.098	0.120±0.120
CRUTEM4.6	0.101±0.012	0.192±0.024	0.279±0.042	0.236±0.110	0.106±0.138
GHCNv3	0.103±0.014	0.207±0.026	0.280±0.044	0.224±0.112	0.052±0.118
GISTEMPv3 (250)	—	0.195±0.026	0.272±0.046	0.241±0.108	0.090±0.122
GISTEMPv3 (1200)	0.098±0.010	0.185±0.020	0.227±0.036	0.203±0.098	0.093±0.120
Berkeley SAT	0.106±0.014	0.194±0.026	0.285±0.048	0.246±0.114	0.161±0.164

Table 3. Century-scale trends in annual global ST change from different datasets（°C / decade）

	1900-2017	1951-2017	1979-2017	1998-2017	1998-2012
CMST	0.086±0.008	0.133±0.014	0.164±0.026	0.190±0.072	0.091±0.088
HadCRUT4	0.079±0.008	0.120±0.016	0.174±0.026	0.147±0.074	0.055±0.094
NOAAGlobalTemp	0.085±0.008	0.138±0.014	0.165±0.024	0.175±0.066	0.084±0.080
GISSv3 (250)	0.078±0.006	0.121±0.014	0.151±0.024	0.134±0.066	0.036±0.080
GISSv3 (1200)	0.086±0.008	0.136±0.014	0.177±0.026	0.154±0.072	0.071±0.094
BE1	0.082±0.006	0.116±0.016	0.188±0.028	0.183±0.074	0.110±0.102
BE2	0.090±0.008	0.130±0.016	0.166±0.026	0.163±0.070	0.079±0.094
ERA5	—	—	0.180±0.032	0.223±0.086	0.140±0.112
HadCRUT Hybrid	—	—	0.189±0.026	0.183±0.070	0.120±0.098

Table 4. Century-scale trends in global, Hemispheric and Tropical Belt ST change（°C / decade）

	1900-2019	1951-2019	1979-2019	1998-2019	1998-2012
NH	0.099±0.011	0.165±0.022	0.248±0.036	0.258±0.086	0.134±0.102
SH	0.077±0.006	0.113±0.011	0.079±0.020	0.125±0.055	0.041±0.098
Tropical Belt	0.081±0.009	0.130±0.018	0.147±0.034	0.186±0.098	0.072±0.165

Table 5. GMST change trends (different uncertainties evaluation) with different SST datasets（°C / decade）

	Uncertainties	1900-2019	1951-2019	1979-2019	1998-2019	1998-2012
Merge1 (CMST)	Fitting	0.091±0.008	0.145±0.014	0.173±0.026	0.195±0.063	0.091±0.088
	Fitting+data	0.091±0.011	0.145±0.019	0.173±0.033	0.194±0.083	0.091±0.094
Merge2	Fitting	0.089±0.010	0.141±0.019	0.209±0.031	0.182±0.074	0.069±0.106
	Fitting+data	0.089±0.012	0.140±0.025	0.208±0.035	0.182±0.094	0.069±0.115

List of Figures

Figure 1 The flowchart of the approach of calculating data uncertainty.

Figure 2 The GLSAT anomaly series and its 95% confidence uncertainty range (a: GLSAT with the error ranges); b: GLSAT series without the error ranges. The anomaly is relative to the 1961-1990 period.

Figure 3 Distribution of the linear trends of SAT in all grid boxes for different datasets (a. C-LSAT; b. CRUTEM4.6; c. GHCNv3; d. GISTEMPv3 (250km); e. GISTEMPv3 (1200km); f. Berkeley SAT. Unit: 0.1 °C/decade)

Figure 4 Annual mean LSAT anomalies (°C) and the linear trends during 1998–2012 (2017) in Arctic (a) and in Globe (b) (relative to 1961-1990)

Figure 5 The distribution of the linear trends of ST in all grid boxes during 1998-2012 for different datasets (a. CMST; b. HadCRUT4; c. NOAAGlobalTemp; d. BE1; e. BE2; f. GISSv3 (1200); g. GISSv3 (250); h. HadCRUT Hybrid; i. ERA5. Unit: 0.1 °C/decade)

Figure 6 Global mean ST anomalies (°C) during 1998–2012 for 8 different datasets (the anomalies of ERA5/HadCRUT Hybrid (dashed lines) are relative to 1979-1990, the rest are relative to 1961-1990)

Figure 7 Comparisons of the global mean ST change series between CMST and other 5 existing datasets.

Figure 8 Gobal (a), North Hemispheric (b), South Hemispheric (c) and Tropics (d) annual mean ST anomalies (°C) during 1900-2017 in CMST (the dashed line are linear trends)

Figure 9 Comparisons of global mean ST change merged with ERSSTv5 and median of HadSST3 (a. ST change series; b. the differences)

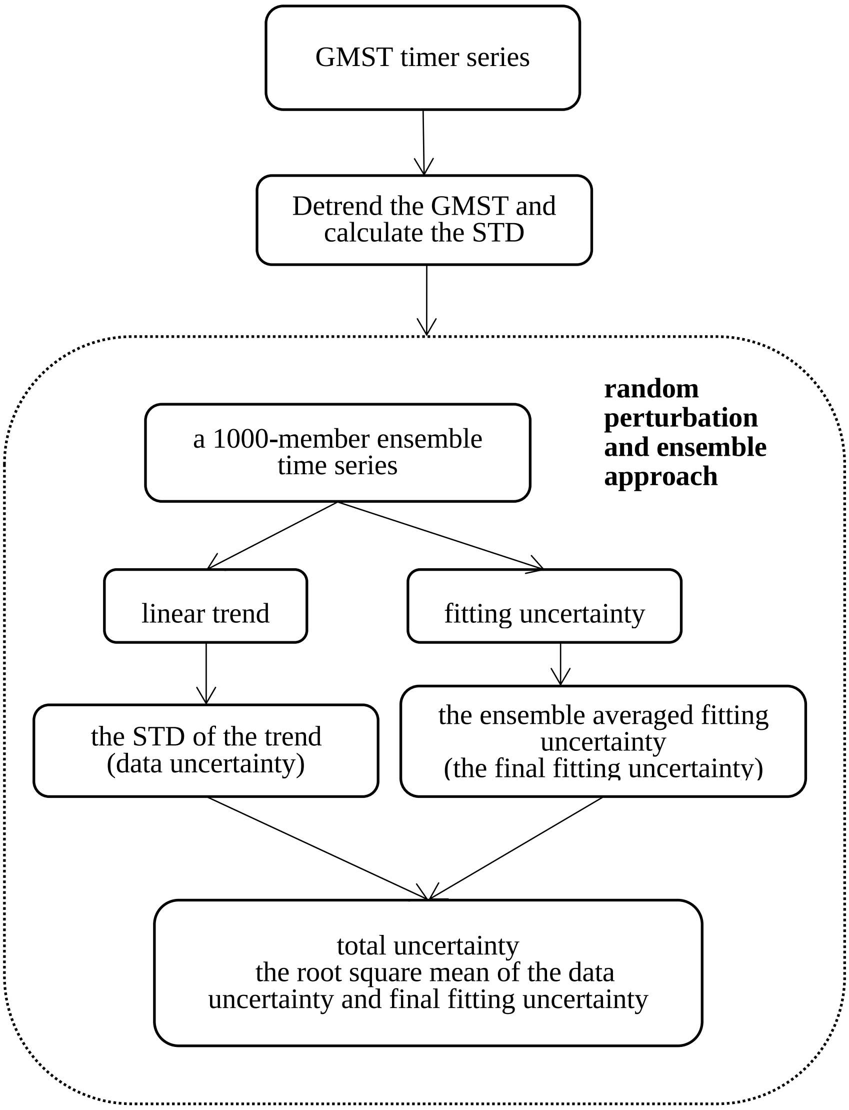

Figure 2 The flowchart of the approach of calculating data uncertainty.

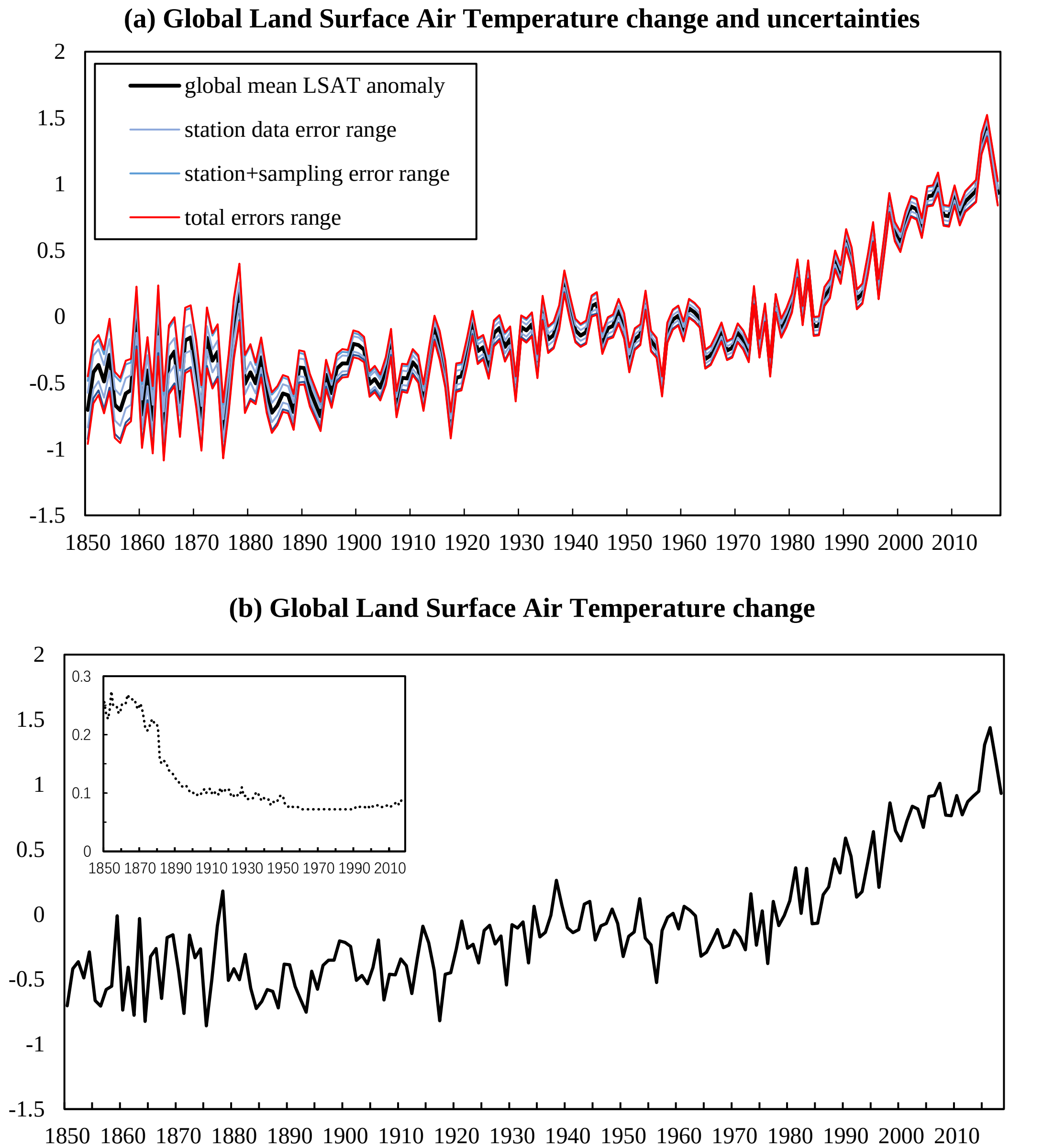

Figure 2 The GLSAT anomaly series and its 95% confidence uncertainty range (a: GLSAT with the error ranges); b: GLSAT series without the error ranges. The anomaly is relative to the 1961-1990 period. The inset in the upper panel shows the uncertainty ranges from different types of errors; and the inset in the lower panel shows the time series of the total error range.

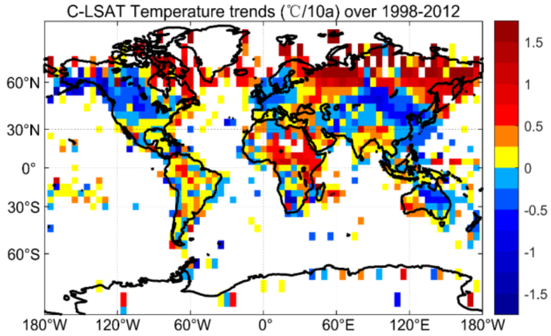

(a)

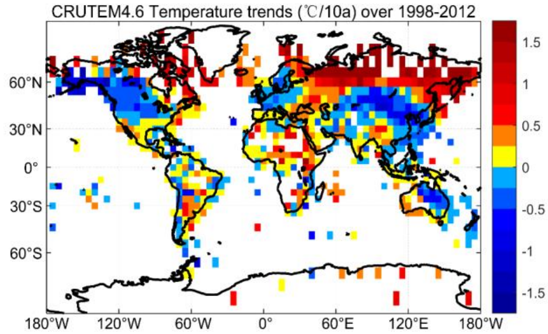

(b)

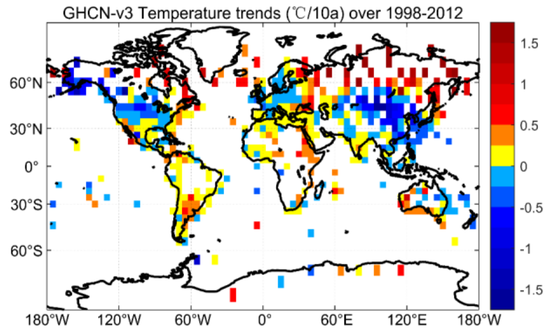

(c)

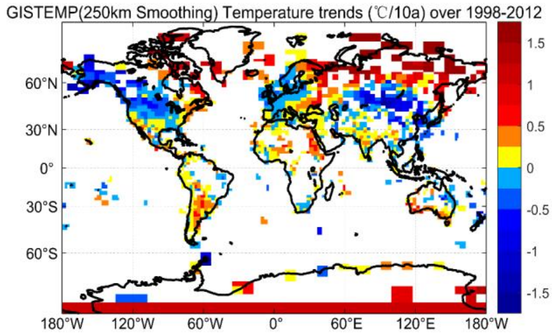

(d)

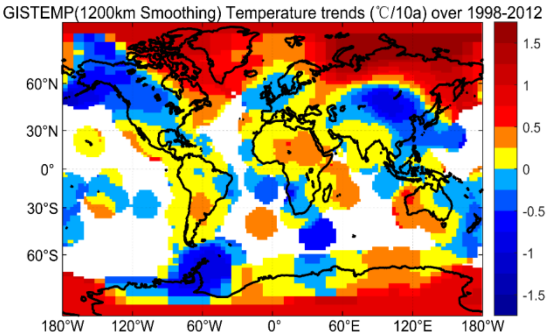

(e)

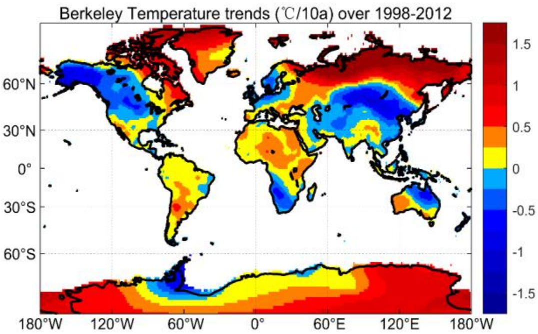

(f)

Figure 3 Distribution of the linear trends of SAT in all grid boxes for different datasets (a. C-LSAT; b. CRUTEM4.6; c. GHCNv3; d. GISTEMPv3 (250km); e. GISTEMPv3 (1200km); f. Berkeley SAT. Unit: 0.1 °C/decade)

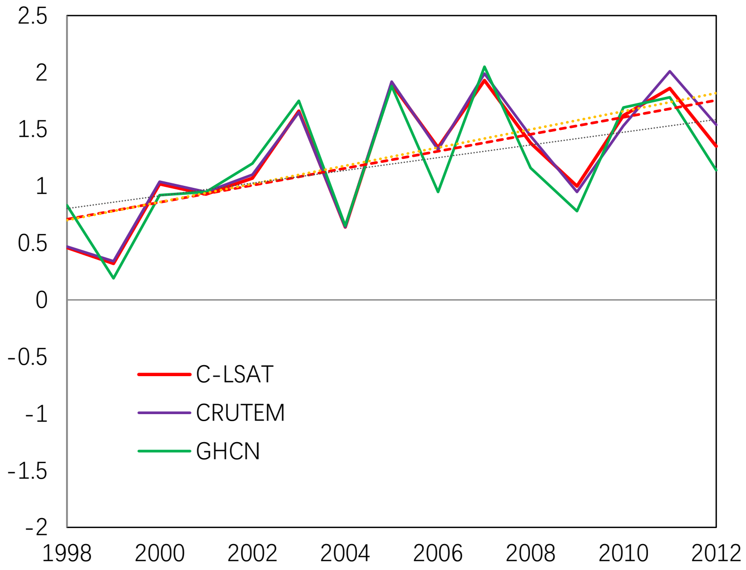

(a)

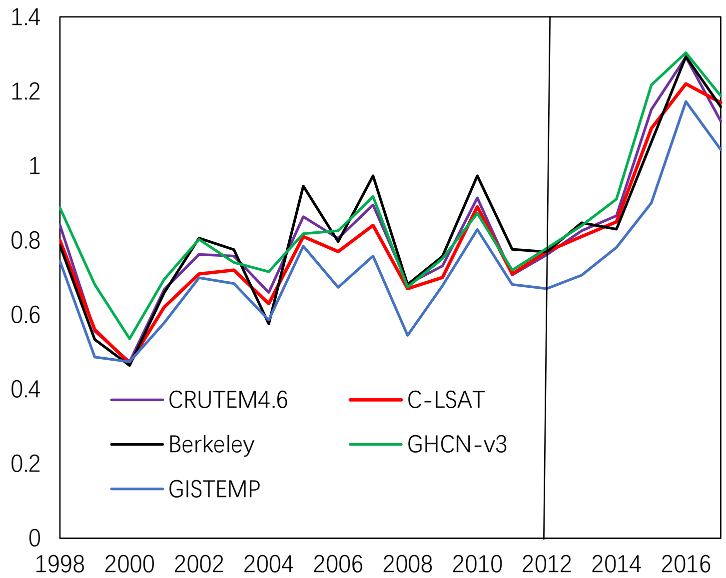

(b)

Figure 4 Annual mean LSAT anomalies (°C) during 1998–2012 (2017) in Arctic (a) and in Globe (b) (relative to 1961-1990)

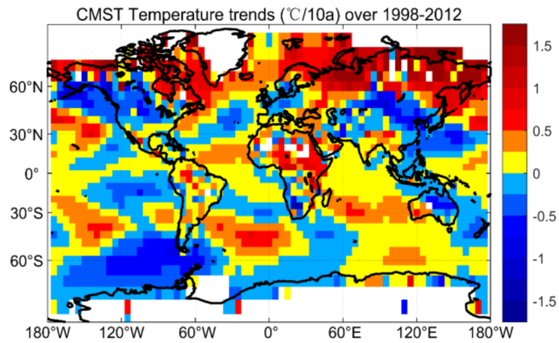
CMST Temperature trends (℃/10a) over 1998-2012
60°N
30°N
0°
30°S
60°S
180°W
120°W
60°W
0°
60°E
120°E
180°W
1.5
1
0.5
0
-0.5
-1
-1.5

(a)

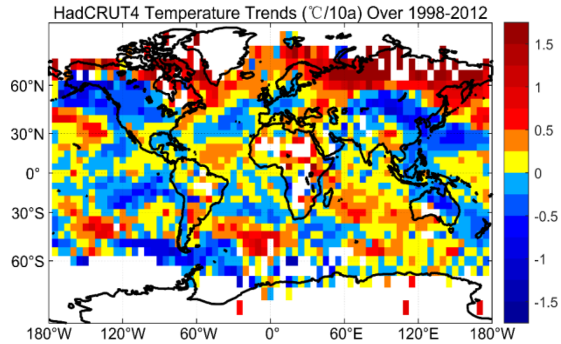
HadCRUT4 Temperature Trends (℃/10a) Over 1998-2012
60°N
30°N
0°
30°S
60°S
180°W
120°W
60°W
0°
60°E
120°E
180°W
1.5
1
0.5
0
-0.5
-1
-1.5

(b)

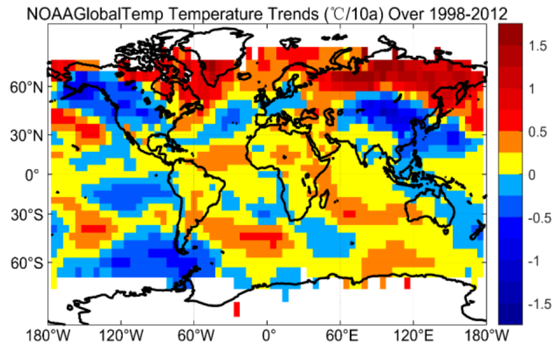
NOAAGlobalTemp Temperature Trends (℃/10a) Over 1998-2012
60°N
30°N
0°
30°S
60°S
180°W
120°W
60°W
0°
60°E
120°E
180°W
1.5
1
0.5
0
-0.5
-1
-1.5

(c)

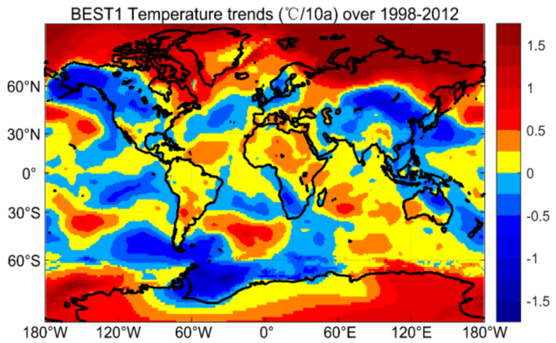
BEST1 Temperature trends (℃/10a) over 1998-2012
60°N
30°N
0°
30°S
60°S
180°W
120°W
60°W
0°
60°E
120°E
180°W
1.5
1
0.5
0
-0.5
-1
-1.5

(d)

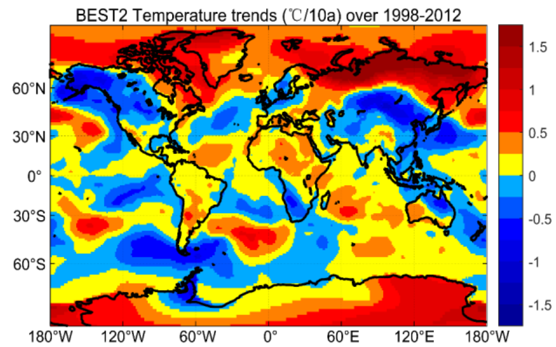
BEST2 Temperature trends (℃/10a) over 1998-2012
60°N
30°N
0°
30°S
60°S
180°W
120°W
60°W
0°
60°E
120°E
180°W
1.5
1
0.5
0
-0.5
-1
-1.5

(e)

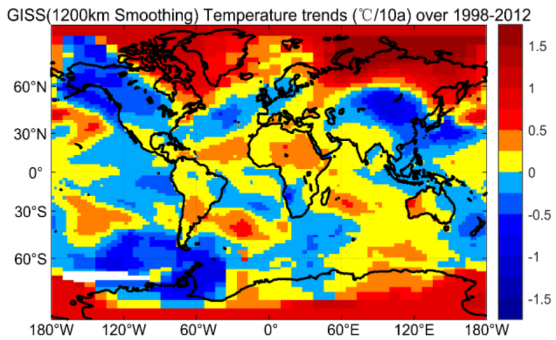
GISS(1200km Smoothing) Temperature trends (℃/10a) over 1998-2012
60°N
30°N
0°
30°S
60°S
180°W
120°W
60°W
0°
60°E
120°E
180°W
1.5
1
0.5
0
-0.5
-1
-1.5

(f)

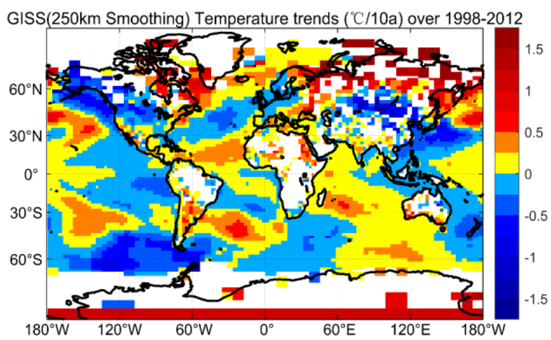
GISS(250km Smoothing) Temperature trends (℃/10a) over 1998-2012
60°N
30°N
0°
30°S
60°S
180°W
120°W
60°W
0°
60°E
120°E
180°W
1.5
1
0.5
0
-0.5
-1
-1.5

(g)

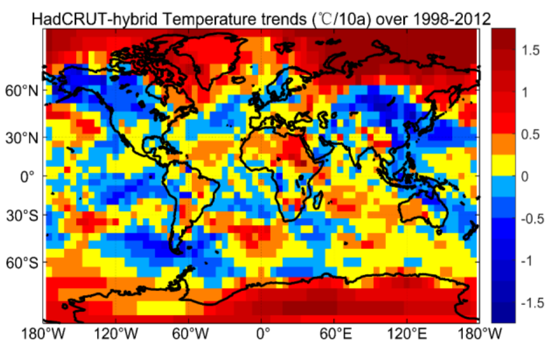
HadCRUT-hybrid Temperature trends (℃/10a) over 1998-2012
60°N
30°N
0°
30°S
60°S
180°W
120°W
60°W
0°
60°E
120°E
180°W
1.5
1
0.5
0
-0.5
-1
-1.5

(h)

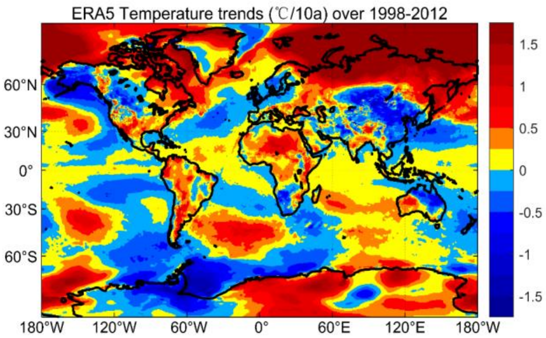

(i)

Figure 5 The distribution of the linear trends of ST in all grid boxes during 1998-2012 for different datasets (a. CMST; b. HadCRUTEM4; c. NOAAGlobalTemp; d. BE1; e. BE2; f. GISS (1200); g. GISS (250); h. HadCRUT Hybrid; i. ERA5. Unit: 0.1 °C/decade)

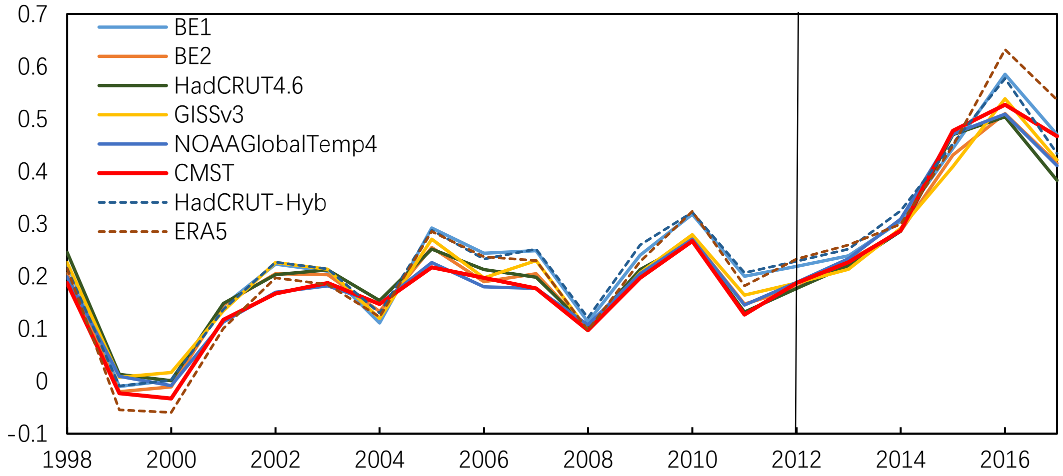

Figure 6 Global annual mean ST anomalies (°C) during 1998–2012 for 8 different datasets (the anomalies are all relative to 1981-2010)

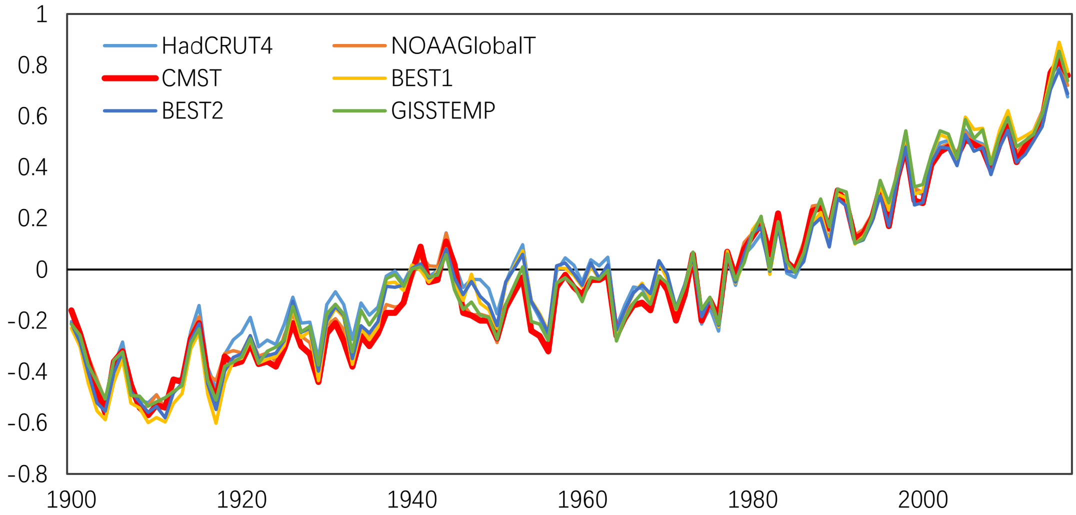

Figure 7 Comparisons of the global mean ST change series between CMST and other 5 existing datasets.

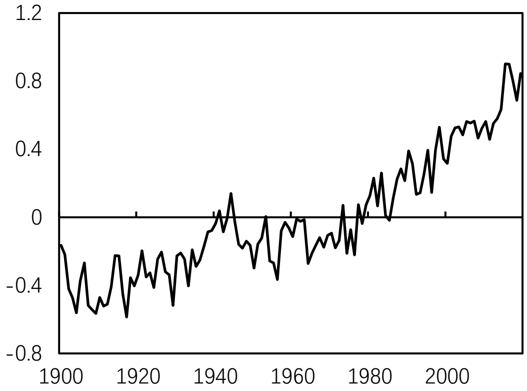

(a)

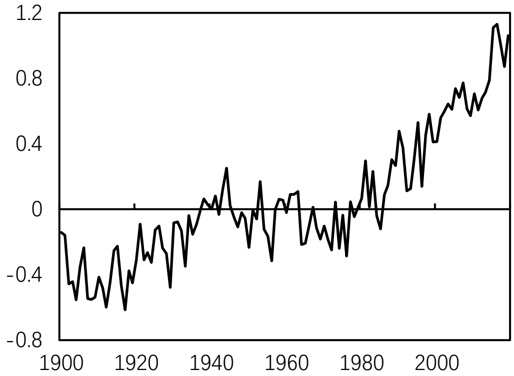

(b)

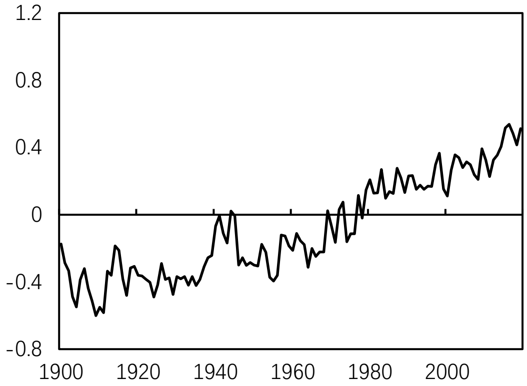

(c)

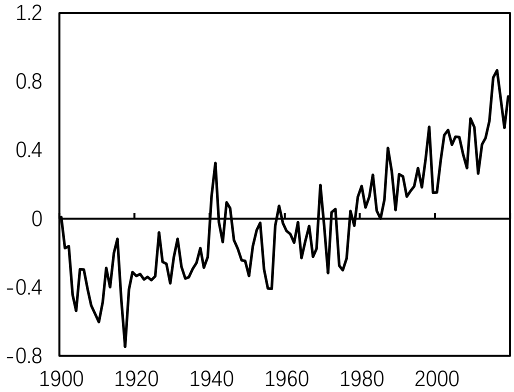

(d)

Figure 8 Global (a), North Hemispheric (b), South Hemispheric (c) and Tropical Belt (d) annual mean ST anomalies (°C) during 1900-2017 in CMST (the dashed lines are linear trends)

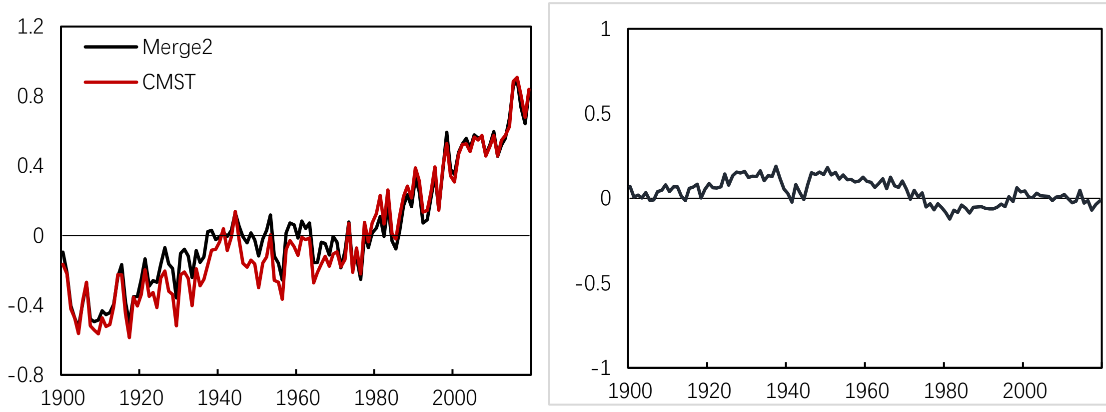

(a) (b)

Figure 9 Comparisons of global mean ST change merged with ERSSTv5 and median of HadSST3

(a. ST change series; b. the differences)